

The Location of the Core in M81

M. F. Bietenholz and N. Bartel

Department of Physics and Astronomy, York University, Toronto, M3J 1P3, Ontario, Canada

and M. P. Rupen

National Radio Astronomy Observatory, Socorro, New Mexico 87801, USA

Accepted to the Astrophysical Journal

ABSTRACT

We report on VLBI observations of M81*, the nuclear core-jet source of the spiral galaxy M81, at five different frequencies between 1.7 and 14.8 GHz. By phase referencing to supernova 1993J we can accurately locate the emission region of M81* in the galaxy's reference frame. Although the emission region's size decreases with increasing frequency while the brightness peak moves to the southwest, the emission region seems sharply bounded to the southwest at all frequencies. We argue that the core must be located between the brightness peak at our highest frequency (14.8 GHz) and the sharp bound to the southwest. This narrowly constrains the location of the core, or the purported black hole in the center of the galaxy, to be within a region of ± 0.2 mas or ± 800 AU (at a distance of ~ 4 Mpc). This range includes the core location that we determined earlier by finding the most stationary point in the brightness distribution of M81* at only a single frequency. This independent constraint therefore strongly confirms our earlier core location. Our observations also confirm that M81* is a core-jet source, with a one-sided jet that extends to the northeast from the core, on average curved somewhat to the east, with a radio spectrum that is flat or inverted near the core and steep at the distant end. The brightness peak is unambiguously identified with the variable jet rather than the core, which indicates limitations in determining the proper motion of nearby galaxies and in refining the extragalactic reference frame.

Subject headings: galaxies: individual (M81) — galaxies: nuclei — radio continuum: galaxies

1. Introduction

The nearby galaxy M81 (NGC 3031, 0951+693) is a grand-design spiral which shares some characteristics with radio galaxies and quasars (Bietenholz et al. 1996, Paper I hereafter). At a distance of ~ 4 Mpc (Freedman et al. 1994; Ferrarese et al. 2000; Bartel & Bietenholz 2003), M81 has the distinction of being the nearest spiral galaxy to have an AGN, with the only nearer AGN being that in the elliptical galaxy Cen A (Israel 1998). The nuclear radio source of M81, which we call M81*, has an average brightness temperature of $\sim 2 \times 10^{10}$ K at 8.4 GHz and a slightly inverted synchrotron spectrum, both typical of radio galaxy cores and quasars. In particular, its radio spectral index, α , ($S_\nu \propto \nu^\alpha$, where S is the flux density and ν the frequency), is about +0.3 from a frequency of ~ 1 GHz to its estimated turnover frequency of ~ 200 GHz (Reuter & Lesch 1996).

This is the third paper in a series, in which we continue our VLBI studies of M81*. M81* is extremely compact and is close to the resolution limit of a ground-based VLBI array at cm wavelengths. We showed in

Paper I that the size of M81* along its major axis is only 0.18 mas or 700 AU at a frequency of 22 GHz (see also Bartel et al. 1982; Kellermann et al. 1976). It is larger at lower ν with the length of the major axis being approximately proportional to $\nu^{-0.8}$. The orientation also changes, bending from $\sim 40^\circ$ at 22 GHz to $\sim 75^\circ$ at 2.3 GHz. We interpreted this structure as being due to a core-jet morphology (Paper I). Even with space VLBI, the morphology of M81* was not completely resolved (Bartel & Bietenholz 2000). Only precision astrometry and the determination of the dynamics and kinematics of different parts of the source allowed the structure to be unambiguously determined and enabled us to show that M81* consists of a stationary core with a one-sided jittery jet to the northeast (Bietenholz, Bartel & Rupen 2000, Paper II hereafter; also Bietenholz, Bartel & Rupen 2001),

M81* also has similarities to the central source in our own Galaxy, Sgr A*, whose radio spectrum is qualitatively very similar, being slightly inverted up to a turn-over frequency. Sgr A* is much smaller than M81* and may represent a version of M81* scaled down in power and size. However, Sgr A* is largely hidden behind scattering clouds of gas that have so far allowed only the crudest determinations of its intrinsic size and orientation (e.g., Bower et al. 2004; Doeleman et al. 2001). M81*, by contrast, is virtually unaffected by scatter broadening at most radio frequencies and it may therefore serve as a more readily observable analog to Sgr A*.

In this paper, we use multi-frequency astrometry to constrain the location of the core of M81*. In general, identifying the core in a radio image of an AGN is a challenge. The most reliable method is to determine astrometrically which component is stationary relative to a physically unrelated source that can be assumed to be stationary on the sky. This method has previously been used for only two sources, the superluminal quasar 3C 345 (Bartel et al. 1986) and the double quasar 1038+528A, B (Rioja & Porcas 2000), although it has also been used to identify a jet component in 4C 39.25 (Guirado et al. 1995).

In the absence of kinematic information, the core is usually identified on the basis of the radio spectrum. Radio emission from a core-jet source is synchrotron emission, and most such sources have a flat or inverted spectrum near the core and steeper spectra farther along the jet. Near the core, the optical depth is high because of synchrotron self-absorption, hence the spectrum tends to being inverted, while farther along the jet, the optical depth is low and the spectrum steep. Another way of identifying the core, then, is by the region of flattest spectrum. Such an identification requires that the images at different frequencies be aligned to an accuracy better than the resolution. This can be done if accurate relative astrometry to a nearby, unrelated source is available, as in cases like 3C 345 and 1038+528 above. In the absence of accurate astrometry, assumptions need to be made, for instance that a particular peak in the brightness distribution at one frequency corresponds with that at another. In some cases, for instance that of 2021+614 (Bartel et al. 1984), the brightness distribution consists of several distinct components and essentially unambiguous alignment is possible. In many other cases, however, the alignment is problematic, particularly close to the core where a frequency dependent morphology is expected due to opacity changes (e.g., Lobanov 1998). In the case of the double quasar 1038+528 a shift in the position of the brightness peak with frequency was in fact measured (Marcaide et al. 1985).

Like many other AGN, the morphology of M81* is simple, and separate components are not clearly discernible. The alignment of the VLBI images of M81* at different frequencies for the purpose of identifying the regions with flat or inverted spectra is impossible without accurate astrometrical information. The coordinates of M81*, therefore, need to be accurately determined at different radio frequencies. In this paper we report on the location of the radio emission region in M81* at five different frequencies spanning an order of magnitude. The effective source size decreases with increasing frequency (Paper I), so at higher frequency, the emission region is smaller, and hence more accurately constrains the core position, if we make

the reasonable assumption that the core is in fact within the emission region. Closely related to this study is the computation of a spectral index image of M81*. However, since M81* is rapidly time-variable, we defer the subject of its time-variable radio spectral index distribution to a forthcoming paper.

The observations of M81* were carried out in conjunction with our ongoing VLBI observations of SN 1993J, for which M81* is used as a phase reference. Our first paper (Paper I) reported on the extremely small size of M81* and its orientation, and their frequency dependence. Our second paper (Paper II) reported on the kinematics and the identification of a stationary core and a one-sided jittery jet in M81*. In this paper we continue our series by using multifrequency astrometry to tightly constrain the core location in a manner largely independent from the study in Paper II.

We describe our observations in § 2, and show representative images of M81* in § 3. We elaborate on the use of SN 1993J as an astrometric reference source in § 4, and determine the location of the emission region as a function of frequency in § 5. We elaborate on the resulting tight constraints on the location of the core in § 6, discuss our results in § 7, and give a summary of our conclusions in § 8.

2. Observations

As mentioned, M81* was observed as a phase reference source for the continuing multi-frequency program of VLBI observations of SN 1993J. We repeat a brief description of the observations here for the convenience of the reader. A more complete description is given in Bartel et al. (2002). We report here on the 32 epochs of VLBI observations completed in mid-2003, made with a global array of between 11 and 18 telescopes with a total time of 12 to 18 hours for each run, giving us exceptionally good $u-v$ coverage. Each telescope was equipped with a hydrogen maser as a time and frequency standard. The data were recorded with the VLBA (Very Long Baseline Array) and either the MKIII or the MKIV VLBI system with sampling rates of 128 or 256 Mbits per second. In each session, data at one or more frequencies of a total of five (14.8, 8.4, 5.0, 2.3, and 1.7 GHz) were recorded, with 8.4 and 5.0 GHz being the standard frequencies used in almost every session. (There were additional observations of SN 1993J but not M81 at 14.8 and 22 GHz, which are not included in this paper.) The VLBI data were correlated using the VLBA processor in Socorro, NM. Further data reduction, i.e., initial calibration, editing, and fringe-fitting, was done with NRAO’s software package, AIPS.

3. Images of M81*

In Figure 1 we show three representative images of M81* taken on 1996 December 13, at frequencies of 8.4, 5, and 2.3 GHz. At each frequency, M81* has a simple brightness distribution, elongated approximately in the southwest to northeast direction. The structure is slightly asymmetric, being somewhat more extended to the northeast, consistent with our earlier findings in Papers I and II. No sub-components are identifiable in our images. The structure is, however, clearly different at the different frequencies. It can be seen that the effective size and orientation vary with frequency, with both the size and position angle, p.a., (north through east) decreasing with increasing frequency.

4. The Center of SN 1993J as an Astrometric Reference Point

Phase-referencing allowed us to obtain very accurate relative positions for M81* and SN 1993J. The two sources are fortuitously very close on the sky, with a separation of only $\sim 170''$, which has the benefit that many systematic sources of error when determining the relative positions are greatly reduced. SN 1993J, however, is not an ideal reference source: it is extended and it changes with time. In order for it to serve as our positional reference, we must select a particular point in its radio morphology that is stationary on the sky and can be reliably determined at each epoch and frequency.

Fortunately, the morphology of SN 1993J allows the selection of such a stationary reference point. Although SN 1993J is expanding rapidly, it has a well defined shell structure which, in projection, has remained circular to within 3% over the 9 years of observations since the explosion (Bietenholz et al. 2001, 2003; see also Marcaide et al. 1997). This circular structure suggests isotropic expansion about a stationary center. In particular, if the geometric center can be shown to be stationary, i.e., to remain at the position of the explosion center, then it would be an almost ideal reference point, independent of epoch and frequency. We determined the position of the geometric center of SN 1993J by fitting the projection of a three-dimensional spherical shell model directly to the u - v data. By monitoring the position of the center of the shell relative to points in the brightness distribution of M81* at 8.4 GHz, we found both a nominal proper motion of the center and the most stable point in the brightness distribution of M81* (Paper II; Bietenholz et al. 2001). The nominal proper motion is small, and thus the geometric center of the shell virtually coincides with the explosion center, having a proper motion of $< 20.7 \mu\text{as yr}^{-1}$ or 360 km s^{-1} (1σ upper limit).

Is the position of the geometric center of SN 1993J frequency dependent? If the structure of the shell were very different at different frequencies then the geometric center position might be frequency dependent. However, the structure of SN 1993J at 5.0 and 1.7 GHz (Bietenholz et al. 2003) and the radius at 15 GHz (see Bartel et al. 2002) are similar to those at 8.4 GHz. Could small differences between the brightness distributions at the different frequencies still lead to significant frequency dependence of the position of the center? We do not think so: the shell at 8.4 GHz is circular to within 3%, and the position of the center is not significantly affected by brightness asymmetries in the shell (Bietenholz et al. 2001). The shell at the other frequencies is similarly circular and any relatively small differences in the brightness distribution along the ridge of the shell would have an equally insignificant effect on the position determination of the center.

We conclude that the geometric center of our shell model of SN 1993J is stationary within the errors and virtually frequency independent, and is thus an almost ideal astrometric reference point for M81*. We therefore use the geometric center of the shell of SN 1993J as a reference point for each epoch and each frequency and determine the relative coordinates of the images of M81*, whose structure does show pronounced and systematic changes with frequency (e.g., Paper I). We adopt R.A. = $09^{\text{h}} 55^{\text{m}} 24\overset{\text{s}}{.}7747593$, decl. = $69^{\circ} 01' 13\overset{\text{s}}{.}703188$ (J2000) for the coordinates of the explosion center of SN 1993J (see Bietenholz et al. 2001). These coordinates agree with the International Celestial Reference Frame (ICRF) coordinates of SN 1993J (IERS 1999) within the standard errors of the latter. We note however, that our results in the present paper do not depend significantly on any particular choice of the “absolute” position values, but only on the relative positions of M81* and SN 1993J.

We also note that the geometric center of SN 1993J may not be quite stationary, since we did find a nominal proper motion with respect to the core of M81* of $11.4 \pm 9.3 \mu\text{as yr}^{-1}$ ($200 \pm 160 \text{ km s}^{-1}$, Bietenholz et al. 2001). Does this motion need to be taken into account? If the proper motion is really that of the center of SN 1993J, whether due to the galactic rotation of SN 1993J, the motion of SN 1993J’s progenitor, or to anisotropy in the expansion, it would affect our results on the relative position determinations of M81*,

since we would then be using a moving reference point. However, since the nominal proper motion is small, being equivalent to a displacement of only 0.10 (± 0.08) mas over our nine-year observing period, the effect would be small also. Further, since our present results are based on time-averages, any effect of the nominal proper motion of SN 1993J’s geometric center would be even less than 0.10 mas and thus not significant.

5. The Radio Emission Region as a Function of Frequency

Armed with the geometric center of SN 1993J as an astrometric reference point, we can proceed to accurately determine the position of points in the brightness distribution of M81*. First we examine how the emission region of M81* varies as a function of frequency. Since the source is only partially resolved, we characterized the emission region by fitting elliptical Gaussians, with the fitting done in the u - v plane. We fitted elliptical Gaussians at each epoch and frequency. The center of the fitted Gaussian is virtually coincident with the peak brightness point discussed below¹. At each frequency, the fitted Gaussian varies with epoch, with the fractional rms variation of the major axis being $\sim 25\%$, and the rms variation in the p.a. being $\sim 10^\circ$. We discussed the temporal variability at 8.4 GHz in Paper II, and we defer a detailed discussion of the temporal variability at other ν to a future paper. For our present purposes, we only require an overall description of the emission region, and a more complicated model, such as that used in Paper II, is not necessary. In Figure 2 we plot the 50% contour of the average elliptical Gaussian at each frequency. It can be seen that the southwest extremity of the 50% contour is roughly coincident at all frequencies, while the northeast one varies considerably, being ~ 2 mas farther to the northeast at 1.7 GHz than at 14.8 GHz.

The correspondence of the southwest 50% points of the average fitted Gaussians at the different frequencies suggests that the actual emission region has a sharp boundary to the southwest which is independent of frequency. A one-sided jet is suggested, with the core being near this 50% point, and the jet extending to the northeast. The extent of the emission to the northeast, or the length of the jet, is roughly proportional to $\nu^{-0.8}$, consistent with our findings in Paper I.

How does the location of the brightness peak vary with frequency? In Table 1 we give the positions of the brightness peak of M81* with respect to the position of the center of SN 1993J’s shell. For easier reading, we tabulate the positions as offsets from the core position derived in Bietenholz et al. (2001), namely R.A. = $09^h 55^m 33.173063$ and decl. = $69^\circ 03' 55'' 061464$ (J2000).

We adopt constant standard errors at each frequency. A detailed discussion of the astrometric uncertainties at 8.4 GHz can be found in Paper II and Bietenholz et al. (2001), and at that frequency we adopt the standard error of 40 μ as used there. The uncertainties at our other frequencies are scaled with ν from the value at 8.4 GHz, with the exception of those at 14.8 GHz, for which a somewhat higher value is taken because of the generally smaller VLBI arrays and thus poorer u - v coverage at that frequency.

We plot the position of the brightness peak at each epoch and frequency in Figure 3. The position of the brightness peak in M81* is somewhat variable at each frequency, as we had already found for 8.4 GHz in Paper II. However, a clear picture emerges when all the points are considered. At each frequency, we determined the average position of the brightness peak. These average positions are also plotted in Figure 3 and listed in Table 2. It is clear that the average position of the brightness peak is a well-behaved function of ν , lying farther to the northeast for lower ν (see Ebbers et al. 1998 for a preliminary version of this result).

¹While the center of the fitted Gaussian is not formally identical to the peak brightness point of an arbitrary brightness distribution, they are coincident to within a small fraction of the positional uncertainties for our data.

The positions of the brightness peak as a function of ν lie along a curved line on the sky, with the p.a. of the line being $\sim 55^\circ$ at the higher frequencies, and changing to $\sim 90^\circ$ by 1.7 GHz. In other words, the emission region in M81* is, on average, bent somewhat to the east, with the emission at high frequencies coming predominately from the southwest. This is consistent with the change in p.a. with frequency observed earlier (Bartel et al. 1982; Paper I), but gives a clearer picture of the jet geometry.

6. The Position of the Core

We have shown that the emission region seems to be sharply bounded, independent of frequency, to the southwest, and that both the size of the emission region and the position of the brightness peak are functions of frequency, with the size increasing and the brightness peak moving to the northeast with decreasing frequency.

In Papers I and II, we showed that M81* could be interpreted as a source with a core and a one-sided jet. In such sources, the radio spectrum is typically flat or inverted near the core where the source is optically thick due to synchrotron self-absorption, and steep farther along the jet where the source becomes optically thin. Such a source produces precisely the frequency-dependent morphology seen in M81*, with the brightness peak moving closer to the core with increasing frequency. The coincidence of the southwest 50% points at different frequencies suggests that any counterjet is indeed faint in comparison to the jet, and thus that the core is near the southwest 50% point. By assuming that the core is within, or at least on the edge of the emission region, we can then use the emission region at our highest frequency of 14.8 GHz, which is the smallest and the most accurately located, to set a fairly small range of possible core locations.

As a conservative estimate of the emission region at 14.8 GHz, we take the 10% contour (rather than the 50% contour plotted earlier) of the average fitted Gaussian to delimit the emission region at that wavelength. That average fitted Gaussian² had a major axis of 0.4 ± 0.1 mas, a minor axis of $0.2^{+0.1}_{-0.2}$ mas (both FWHM) and p.a. of $41 \pm 13^\circ$. The 10% contour of that Gaussian is also plotted in Figure 3.

Since the size of the emission region decreases and the position of the brightness peak moves to the southwest with increasing frequency over our entire 10 to 1 frequency range, it seems reasonable to assume that this behavior would continue to even higher frequencies, perhaps even to ~ 200 GHz where the integrated spectrum begins to steepen (Reuter & Lesch 1996). If we assume that the core is located within the emission region, and near the brightness peak, at such high frequencies, then the core location must be to the southwest of the brightness peak even at our highest frequency of 14.8 GHz.

Combining these two constraints, namely that the core be within the emission region at 14.8 GHz and that it be southwest of the brightness peak at that same frequency, allows us to tightly constrain the region where the core could be located, indicated by the shaded half-ellipse drawn in Figure 3. Our earlier determination of the core position in Paper II and Bietenholz et al. (2001), which is also plotted in Figure 3, falls very near the center of this region of possible core positions.

Since the location of brightness peak seems to be a well-behaved function of frequency, or correspondingly of the observing wavelength, λ , one could extrapolate this function to $\lambda = 0$, or perhaps at least to $\lambda \sim 1$ mm (i.e., $\nu \sim 200$ GHz) where the integrated spectrum turns over, and use the extrapolated position as an

²The uncertainties given are standard deviations over five observing epochs, representing both the measurement uncertainties and intrinsic variation of the size and orientation of the radio source.

estimate of the core position. Such an extrapolation, however, requires knowledge of the functional form of the dependence of the position on λ . Neither the physics of the radio emission or the jet geometry are well known enough to determine a particular choice for this function. As an illustrative example, we chose a simple linear function of λ , which we fit by weighted least-squares to both the R.A. and the decl. of the brightness peak for our three shortest wavelengths, those being the ones closest to the core and therefore providing the most useful constraints on the core position. Since only a relatively small extrapolation is required between our shortest observed wavelength of $\lambda = 2.0$ cm and $\lambda = 0$, we think that our extrapolation is reasonable despite being non-unique. The intercept of these fits give us a position at $\lambda = 0$ of R.A. = $09^{\text{h}} 55^{\text{m}} 33.173087$ and decl. = $69^{\circ} 03' 55.061603$ (J2000), which we also plot in Figure 3 (\otimes). This position is less than 75 μ as away from the core position derived in Paper II, and thus well within the uncertainties of the latter.

7. Discussion

Using VLBI observations of M81* at 32 epochs and at a total of five frequencies, all phase-referenced to a physically unrelated source in the same galaxy (SN 1993J), has allowed us to place tight constraints on the location of the core, showing it must be within a region of about ± 0.2 mas of the southwestern part of the brightness distribution at our highest frequency of 14.8 GHz. This is consistent with the position of the core we derived earlier by finding the most stable point within the radio morphology of M81* (Paper II). Furthermore the constraints on the core location are of comparable size to the uncertainties of the earlier core position.

The present finding provides an important independent confirmation of our earlier core location. Although the determination of the core position from Paper II was obtained from a subset of the observations used for the present one, our present results are largely independent of the earlier core position, since that earlier position was based on the time-variability of the morphology of M81* at only one frequency. The present results, by contrast, are based upon a time-average of the peak position at different frequencies. Any possible errors in the astrometry would seem unlikely to affect the two determinations of the core position in the same manner.

The positions of the brightness peak at different frequencies, plotted in Figure 3, also draw a clear picture of the average jet geometry, with the jet extending to the northeast of the core, and being bent somewhat to the east. This bending is consistent with what was found in Bartel et al. (1982) and Paper I. However, we showed in Paper II that the geometry of M81*, at least at 8.4 GHz, was intrinsically variable: between 1993 and 1998, the FWHM major axis size varied between 0.40 and 0.70 mas and its p.a. between 44° and 57° . This variability is reflected in the scatter of the brightness peak positions at each frequency in Figure 3. This scatter does not affect our core position, since the core can be assumed stationary, and our core position is derived from the time-averaged positions at each frequency. In any case, the scatter is considerably smaller than the variation of the peak position with frequency from which our core position is derived.

In general, the identification of the core will be important for unambiguously determining the spectral index distribution of M81*, for instance to determine the spectral index distribution of the jet. Further, the identification of the core, as we noted in Paper II, is important for efforts to determine the proper motion of the galaxy M81 in the extragalactic reference frame.

Finally the independent confirmation of the core position to within the latter's uncertainties strongly

supports our identification of the explosion center of SN 1993J, the small limits on the proper motion of SN1993J's geometric center, and the near isotropy of its expansion (Bietenholz et al. 2001, 2003).

7.1. The Spectral Index Distribution of M81*

The results described in this paper imply a strong gradient in the radio spectral index of M81*, since if the spectral index were uniform, then the morphology would be similar at different frequencies and no displacement of the brightness peak as a function of frequency would be seen. The gradient is such that the spectrum near the core is flatter than that at the far end of the jet. We estimate that $\alpha \gtrsim 0.0$ near the core, and $\alpha \sim -0.7$ along the jet ~ 1 mas away from the core. We will discuss the spectral index distribution of M81* in detail in a future paper.

7.2. The Extragalactic Reference Frame

In general, our results indicate limitations to the accuracy of the extragalactic reference frame as determined with VLBI observations. Most of the sources defining the ICRF extragalactic reference frame (Ma et al. 1998; IERS 1999) have core-jet structure, which often shows some variability with time (Fey, Clegg, & Fomalont 1996; Fey & Charlot 1997, 2000; Gontier et al. 2001), due presumably to a variable jet. The most accurate determination of the extragalactic reference frame would therefore be obtained by determining the positions of the cores of the reference frame sources. Our results show that, even in a source as compact as M81*, not only does the peak of the brightness distribution not coincide with the core, but also that the position of the peak of the brightness distribution is frequency dependent³.

We note also that an error is made when the effect of the ionospheric delay is computed from simultaneous observations at 8.4 and 2.3 GHz with the assumption that the sources' positions coincide at the two frequencies. Any discrepancy in the position causes an astrometric error of about 7% of the discrepancy. In the case of M81* this error would be about 0.05 mas at 8.4 GHz (we note that it was not necessary to determine the ionospheric delay in this fashion for our relative astrometry, so our position values are unaffected by this error).

However, if the position of the peak in the brightness distribution were stable over time, then it could be taken as an astrometric fixed point for the extragalactic reference frame, without having to locate the core within the brightness distribution. Our finding that the peak position is variable by ~ 0.3 mas at all our frequencies shows that using the brightness peak (or the centroid of the emission region) as a reference point limits the positional accuracy to that level. In the case of M81*, the variability in position is only about one third of the error of the ICRF position. The errors of the positions of some ICRF sources, however, are as small as 0.1 mas. The angular scales on which core-jet structure is seen or expected for the ICRF sources is from 0.1 mas upward. M81* is a very compact source, and since the position of the peak of the brightness distribution is variable on a scale of 0.3 mas it is conceivable that the stability of the positions of even the most compact ICRF sources is limited to about ± 0.1 mas.

³In fact, Da Silva Neto et al. 2002, reported on discrepancies of up to 15 mas between the radio and the optical positions of the ICRF reference frame sources, although it is not clear these discrepancies can be directly attributed to radio source structure.

7.3. The Proper Motion of M81

The dynamics of galaxies of the Local Group and beyond are an important area of research in astronomy. Since a proper motion has not yet been measured for any galaxy, studies of the galaxy dynamics are based exclusively on the radial component of their velocities. The galaxy M81 is one of the few whose proper motion could perhaps be measured in the not so distant future. Observations of the core in M81* relative to quasars nearby on the sky over a period of about 10 years might give the proper motion of the galaxy with a standard error $\lesssim 100 \text{ km s}^{-1}$, since unlike M81*, the cores of the more distant quasars are not expected to display any discernible proper motion (see e.g., Bartel et al. 1986). In fact, since Nagar et al. (2002) have shown that many nearby low-level AGNs have mas-scale cores with brightness temperatures $> 10^8 \text{ K}$, such analysis could be extended to other nearby galaxies.

However, as we point out in § 7.2 above, the intrinsic variability of core-jet sources, including M81* itself, limits the accuracy with which the proper motion of M81* could be determined in this fashion. For the highest accuracy, therefore, one would need repeated observations of M81* together with several reference sources, and an analysis similar to the one we carried out in Paper II and Bietenholz et al. (2001) to locate the cores as most stable points within the brightness distributions of each reference source.

8. Conclusions

1. We determined the size of the emission region of M81* and its location with respect to the geometric center of SN 1993J at five different observing frequencies spanning an order of magnitude.
2. The size of the emission region decreases with increasing observing frequency. The position of the brightness peak shifts progressively toward the southwest extremity with increasing frequency. The position of that southwest extremity is largely frequency-independent, suggesting a hard edge to the emission region at that point.
3. This progressive shift is expected for the emission from a compact core-jet source with a flat or inverted spectrum near the core and a steep spectrum at the far end of the jet, and thus confirms our earlier identification of M81* as a core-jet source.
4. We argue that the core is within the southwest half of the emission region at our highest frequency of 14.8 GHz, which constrains the core to be located within a region of about $\pm 0.2 \text{ mas}$. This constraint is consistent with, but independent from, our earlier determination of the core position, and thus strongly confirms the latter.
5. The confirmation of the core location in M81* also confirms our identification of the explosion center of SN 1993J and its isotropic expansion therefrom.
6. The brightness peak of M81* is unambiguously identified with the jet rather than with the core. The location of the brightness peak relative to the stationary core is variable both in time and with frequency.
7. An accurate location of the core, as opposed to the brightness peak, will be important in determining the proper motion of nearby galaxies in particular, and in refining the extragalactic reference frame in general.

We thank V. I. Altunin, A. J. Beasley, W. H. Cannon, J. E. Conway, D. A. Graham, D. L. Jones, A. Rius, G. Umana, and T. Venturi for help with several aspects of the project. R. Bartel, J. Cadieux, M. Craig, R. Freedman, M. Keleman, and B. Sorathia helped with some aspects of the VLBI data reduction during their tenure as students at York. We thank NRAO, the European VLBI Network, and the NASA/JPL Deep Space Network (DSN) for providing exceptional support for this extended and ongoing observing campaign. We also thank Natural Resources Canada for helping with the observations at the Algonquin Radio Observatory during the first years of the program. Research at York University was partly supported by NSERC. NRAO is operated under license by Associated Universities, Inc., under cooperative agreement with NSF. The European VLBI Network is a joint facility of European and Chinese radio astronomy institutes funded by their national research councils. The NASA/JPL DSN is operated by JPL/Caltech, under contract with NASA. We have made use of NASA's Astrophysics Data System Abstract Service.

REFERENCES

Bartel, N., et al. 1982, *ApJ*, 262, 556

Bartel, N., et al. 1984, *ApJ*, 279, 116

Bartel, N., Herring, T. A., Ratner, M. I., Shapiro, I. I. & Corey, B. E. 1986, *Nature*, 319, 733

Bartel, N., et al. 2002, *ApJ*, 581, 404

Bartel, N., & Bietenholz, M. F. 2003, in Future Directions in High Resolution Astronomy (PASP) *in press*

Bartel, N., & Bietenholz, M. F. 2000, in Proceedings of the VSOP Symposium, eds. H. Hirabayashi, P. G. Edwards, and D. W. Murphy, (Sagamihara: Institute of Space and Astronautical Science), 17

Bietenholz, M. F., et al. 1996, *ApJ*, 457, 604, Paper I

Bietenholz, M. F., Bartel, N., & Rupen, M. P. 2000, *ApJ*, 532, 895, Paper II

Bietenholz, M. F., Bartel, N., & Rupen, M. P. 2001, *ApJ*, 557, 770

Bietenholz, M. F., Bartel, N., & Rupen, M. P. 2003, *ApJ*, 597, 374

Bower, G. C., Falcke, H., Herrnstein, R. M., Zhao, J.-H., Goss, W. M., & Backer, D. C., 2004, *Science*, 304, 704

da Silva Neto, D. N., Andrei, A. H., Vieira Martins, R., & Assafin, M. 2002, *AJ*, 124, 612

Doeleman, S. S., et al. 2001, *AJ*, 121, 2610

Ebbers, A., Bartel, N., Bietenholz, M. F., Rupen, M. P. & Beasley, A. J. 1998, in IAU Colloquium 164: Radio Emission from Galactic and Extragalactic Compact Sources, ed. J. A. Zensus, G. B. Taylor, and J. M. Wrobel (San Francisco: ASP) 203

Fey, A. L., Clegg, A. W., & Fomalont, E. B. 1996, *ApJS*, 105, 299

Fey, A. L., & Charlot, P. 1997, *ApJS*, 111, 95

Fey, A. L., & Charlot, P. 2000, *ApJS*, 128, 17

Freedman, W. L., et al. 1994, *ApJ*, 427, 628

Ferrarese, L., et al. 2000, *ApJS*, 128, 431

Gontier, A.-M., Le Bail, K., Feissel, M., & Eubanks, T. M. 2001, *A&A*, 375, 661

Guirado, J. C., et al. 1995, *AJ*, 110, 2586

IERS. 1999, Ann. Rep., ed. D. Gambis (Paris: Obs. Paris), 87

Israel, F. P. 1998, Astron. and Astrop. Rev. 8, 237

Kellermann, K. I., Shaffer, D. B., Pauliny-Toth, I. I. K., Preuss, E., & Witzel, A. 1976, ApJ, 210, L121

Lobanov, A. P. 1998, A&A Suppl. Ser., 132, 261

Ma, C., Arias, E. F., Eubanks, T. M., Fey, A. L., Gontier, A.-M., Jacobs, C. S., Sovers, O. J., Archinal, B. A., Charlot, P. 1998, AJ, 116, 516

Marcaide, J. M., et al. 1985, A&A, 142, 71

Marcaide, J. M., et al. 1997, ApJ, 486, L31

Nagar, N. M., Falcke, H., Wilson, A. S., Ulvestad J. S., 2002, A&A, 392, 53

Reuter, H.-P., & Lesch, H. 1996, A&A, 310, L5

Rioja, M. J., & Porcas, R. W. 2000, A&A, 355, 552

Table 1. Position Offsets of the Brightness Peak of M81*

Date	Position Offset (mas)									
	14.8 GHz		8.4 GHz		5.0 GHz		2.3 GHz		1.7 GHz	
	$\Delta\alpha^a$	$\Delta\delta^a$	$\Delta\alpha$	$\Delta\delta$	$\Delta\alpha$	$\Delta\delta$	$\Delta\alpha$	$\Delta\delta$	$\Delta\alpha$	$\Delta\delta$
1993 May 16	0.06	0.13	0.10	0.10
1993 Jun 26	0.19	0.12
1993 Sep 18	0.11	0.01	0.14	0.13
1993 Nov 5	0.16	0.24
1993 Dec 16	0.28	0.08
1994 Jan 28	0.18	0.19
1994 Mar 14	0.19	0.27	1.11	0.48
1994 Apr 21	0.22	0.33	0.30	0.38
1994 Jun 21	0.21	0.21	0.33	0.39
1994 Aug 29	0.19	0.20	0.34	0.37
1994 Oct 31	0.17	0.18	0.27	0.35
1994 Dec 23	0.18	0.19	0.37	0.40	0.47	0.40
1995 Feb 12	0.21	0.16
1995 May 10	0.24	0.16	0.36	0.30
1995 Aug 17	0.28	0.25	0.39	0.34
1995 Dec 18	0.24	0.13	0.44	0.28	0.84	0.38
1996 Apr 7	0.30	0.18	0.38	0.24
1996 Aug 31	0.19	0.14	0.36	0.27
1996 Dec 13	0.31	0.19	0.48	0.34	0.79	0.52
1997 Jun 6	0.23	0.17
1997 Nov 14	0.22	0.21	0.30	0.19	0.72	0.42
1998 Jun 3	0.31	0.25	0.39	0.31
1998 Nov 20	0.52	0.33
1998 Dec 7	0.29	0.22	0.74	0.47
1999 Jun 5	1.08	0.49
1999 Jun 16	0.34	0.30
1999 Nov 23	0.57	0.24
2000 Feb 24	0.45	0.16
2000 Nov 12	0.22	0.08
2001 Jun 9	0.49	0.13
2001 Nov 25	1.08	0.26
2002 May 25	0.49	0.10
Standard Error: ^b	0.04	0.04	0.04	0.04	0.07	0.07	0.15	0.15	0.20	0.20

^aThe R.A. (α) and decl. (δ) offsets of the position of the brightness peak of M81* from $9^h 55^m 33^s.173103, 69^\circ 3' 55''061630$ derived in Paper II at 8.4 GHz, determined from astrometry to SN 1993J and taking the center position of SN 1993J to be $9^h 55^m 24^s.7747593, 69^\circ 1' 13''703188$ (J2000)

^bStandard errors, see text §5

Table 2. Average Position of the Brightness Peak of M81* as a Function of Frequency

Frequency (GHz)	$N_{\text{obs}}^{\text{a}}$	Average Position Offset ^b (mas)			
		$\Delta\alpha$	rms_{α}	$\Delta\delta$	rms_{δ}
14.8	2	0.08	0.04	0.07	0.08
8.4	25	0.23	0.07	0.18	0.06
5.0	18	0.39	0.08	0.29	0.09
2.3	5	0.71	0.13	0.48	0.08
1.7	3	1.09	0.02	0.41	0.13

^aThe number of observing epochs at each frequency

^bThe average over all observing epochs of the R.A. (α) and decl. (δ) offsets of the position of the brightness peak of M81* and their rms variation over all of our observing epochs. The offsets in position are from $09^{\text{h}} 55^{\text{m}} 33\text{s}.173103$, $69^{\circ} 03' 55''$ 061630 (J2000)

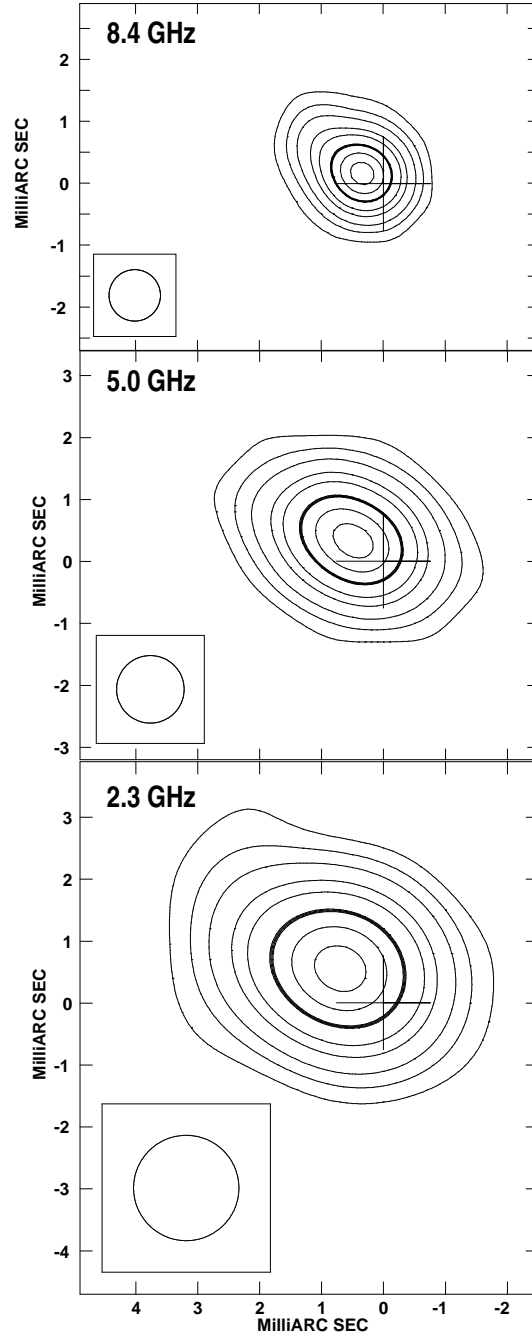


Fig. 1.— Images of M81* on 1996 December 13 at observing frequencies of 8.4, 5.0 and 2.3 GHz. In each panel, the origin of the coordinate system is marked by a cross and is the core position derived in Paper II, the FWHM size of the restoring beam is indicated at lower left, and the contours are drawn at 2, 5, 10, 20, 30, 40, **50** (heavy contour), 70 and 90% of the brightness peak. North is up and east is to the left.

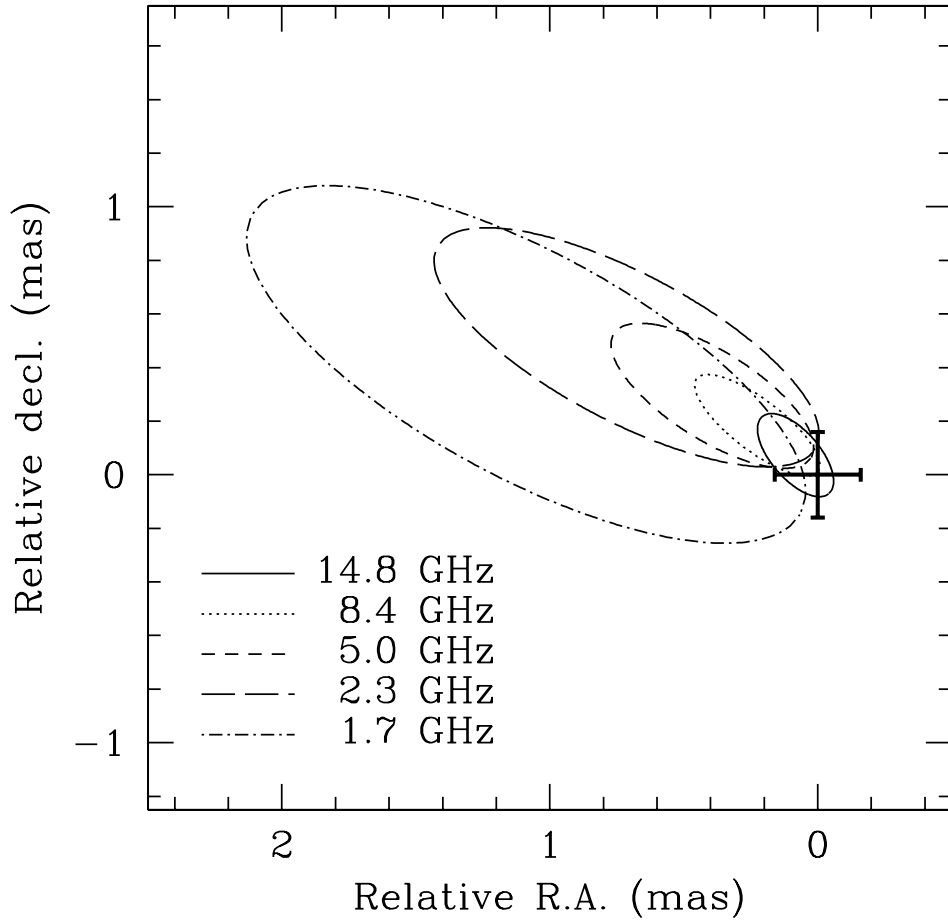


Fig. 2.— The 50% contour of the average over all epochs of the elliptical Gaussians fit to the emission at each frequency. The average elliptical Gaussian at each frequency is formed by averaging separately the R.A. and decl. offsets, the FWHM major and minor axes, and the p.a. of the fitted Gaussians at each epoch. The center position of the Gaussians is determined with respect to the geometric center of SN 1993J. The origin of the coordinate system is the core position determined in Paper II, which is at R.A. = $09^{\text{h}} 55^{\text{m}} 33\overset{\text{s}}{.}173063$, decl. = $69^{\circ} 03' 55\overset{\text{s}}{.}061464$ (J2000), and is indicated, along with its uncertainty, by the cross.

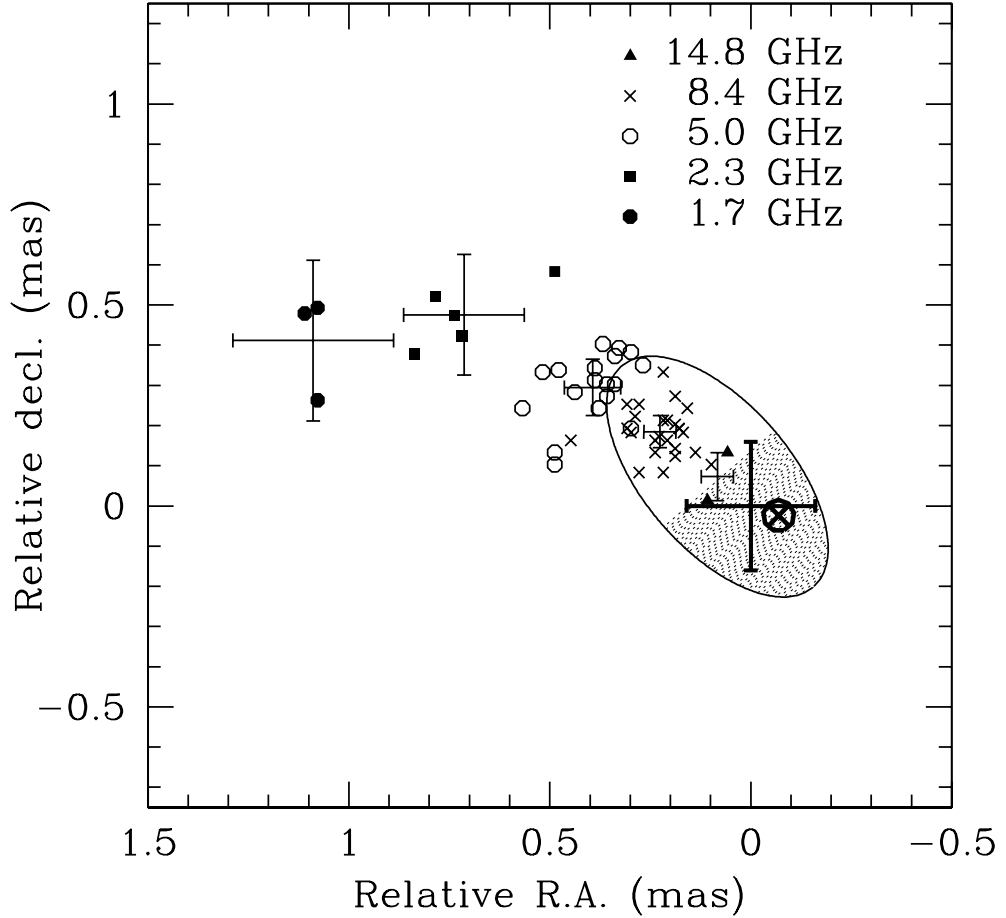


Fig. 3.— The position of the brightness peak of M81* with respect to the geometric center SN 1993J for each epoch of observation. The points show the positions of the peak at each epoch at the frequencies indicated. The estimated standard errors of each measurement in R.A. and decl. are 40, 40, 70, 150 and 200 μ as at frequencies of 14.8, 8.4, 5.0, 2.3 and 1.7 GHz respectively. The thin crosses show the average positions over all epochs at each frequency, with the plotted standard error being the larger of the rms variation in the average position and the positional uncertainty of each individual measurement at that frequency. The heavy cross shows the core position of R.A. = $09^{\text{h}} 55^{\text{m}} 33\rlap{.}^{\text{s}} 173063$, decl. = $69^{\circ} 03' 55\rlap{.}'' 061464$ (J2000; Bietenholz et al. 2001), derived from the variability of the source structure at 8.4 GHz, which we also use as the origin of our coordinate system, with its standard error. The ellipse shows the average extent of the emission at 14.8 GHz or $\lambda = 2.0$ cm (10% contour), with the shaded half indicating a conservative estimate of the range of possible core positions (§ 6). The \otimes shows an extrapolation of the position of the brightness peak to $\lambda = 0$ (see § 6).